Journal of Alloys and Compounds 873 (2021) 159828

Contents lists available at ScienceDirect

Journal of Alloys and Compounds

journal homepage: www.elsevier.com/locate/jalcom

Potassium and thallium conductors with a trigonal structure in the M_2MoO_4–$Cr_2(MoO_4)_3$–$Hf(MoO_4)_2$ (M = K, Tl) systems: Synthesis, structure, and ionic conductivity

Victoria G. Grossman[a,*], Maxim S. Molokeev[b,c,d], Bair G. Bazarov[a], Jibzema G. Bazarova[a]

[a] Baikal Institute of Nature Management, SB RAS, Sakhyanovoy St., 6, Ulan-Ude 670047, Russia
[b] Kirensky Institute of Physics, Federal Research Center KSC, Siberian Branch, Academy of Sciences, 50/38 Akademgorodok, Krasnoyarsk 660036, Russia
[c] Siberian Federal University, 82 Svobodniy Av., Krasnoyarsk 660041, Russia
[d] Department of Physics, Far Eastern State Transport University, Serysheva str. 47, Khabarovsk 680021, Russia

ARTICLE INFO

Article history:
Received 13 February 2021
Received in revised form 23 March 2021
Accepted 30 March 2021
Available online 8 April 2021

Keywords:
Synthesis
Thallium
Potassium
Molybdates
Phase diagram
DSC
Conducting material

ABSTRACT

The triple molybdates $M_5CrHf(MoO_4)_6$ (M = K, Tl) and $TlCrHf_{0.5}(MoO_4)_3$ were found upon studying the corresponding ternary molybdate systems M_2MoO_4–$Cr_2(MoO_4)_3$–$Hf(MoO_4)_2$ (M = K, Tl) in the subsolidus region using X-ray powder diffraction. The crystal structures of $M_5CrHf(MoO_4)_6$ (M = K, Tl) and $TlCrHf_{0.5}(MoO_4)_3$ are refined by Rietveld method. $M_5CrHf(MoO_4)_6$ (M = K, Tl) crystallizes in space group $R\bar{3}c$ with unit cell parameters: $a = b = 10.45548$ (5), $c = 37.24614$ (3) Å, $V = 3526.14$ (4) Å^3, $Z = 6$ for $K_5CrHf(MoO_4)_6$ and $a = b = 10.53406$ (12), $c = 37.6837$ (5) Å, $V = 3621.39$ (9) Å^3, $Z = 6$ for $Tl_5CrHf(MoO_4)_6$. $TlCrHf_{0.5}(MoO_4)_3$ crystallizes in space group $R\bar{3}$ with unit cell parameters: $a = b = 12.9710$ (2), $c = 11.7825$ (2) Å, $V = 1716.78$ (6) Å^3, $Z = 6$. The thermal stability and electrical conductivity of the new compounds were investigated. Electrical conductivity measurements gave high values for the triple molybdates $M_5CrHf(MoO_4)_6$ (M = K, Tl) ($\sigma = 5.22 \times 10^{-4}$ S / cm for $K_5CrHf(MoO_4)_6$, $\sigma = 1.1 \times 10^{-2}$ S / cm for $Tl_5CrHf(MoO_4)_6$ at 773 K) and relatively low values for the triple molybdate $TlCrHf_{0.5}(MoO_4)_3$ ($\sigma = 4.42 \times 10^{-6}$ S / cm at 773 K).

© 2021 Published by Elsevier B.V.

1. Introduction

Complex molybdates containing alkaline elements are interesting in their physical properties and rich crystal chemistry [1–19]. It is known that molybdates with a framework structure were found to undergo polymorphic transformations [20–26]. This leads to a disordered structure with high ionic conductivity. Alkaline ions in these structures are weakly bonded to the ions of the framework and therefore they are conductive. Earlier we synthesized and characterized potassium-, and thallium-containing triple molybdates $K_5RHf(MoO_4)_6$ (R = In, Sc) [25,27], $Tl_5RHf(MoO_4)_6$ (R = Fe, In, Bi) [28–31]. The conductivity of molybdates $M_5RHf(MoO_4)_6$ (M = K, Tl; R = Fe, In, Sc, Bi) is rather high. For example, $K_5ScHf(MoO_4)_6$ demonstrates a conductivity of 2.63×10^{-4} at 773 K, $Tl_5InHf(MoO_4)_6$ – 7.51×10^{-4} at 773 K. We decided to conduct a study of chromium-containing systems due to the fact that systems containing chromium as a trivalent ion have not been studied. Chromium is a metal with very unusual properties. For the most part, its compounds are of interest. To date, a small amount of chromium-containing molybdates has been obtained $Li_3Cr(MoO_4)_3$ [16], $Na_{2x}Zn_2Sc_{2(1-x)}(MoO_4)_3$, $Na_{2x}Cd_2Sc_{2(1-x)}(MoO_4)_3$, $Na_{2x}Mg_2Sc_{2(1-x)}(MoO_4)_3$ [32], $Na_{1-x}Mg_{1-x}Cr_{1+x}(MoO_4)_3$ ($0 \le x \le 0.3$), $NaMg_3Cr(MoO_4)_5$ [33], $KMgCr(MoO_4)_3$ [21], $CsCrZr_{0.5}(MoO_4)_3$ $CsCrTi_{0.5}(MoO_4)_3$ [34,35], $Cs_5CrHf(MoO_4)_6$, $CsCrHf_{0.5}(MoO_4)_3$ [36], $K_5CrZr(MoO_4)_6$ [37], $AgMg_3Cr(MoO_4)_5$ and $AgMn_3Cr(MoO_4)_5$ [38]. Oxide $Li_3Cr(MoO_4)_3$ with a NASICON-type structure has a conductivity of about 10^{-4}–10^{-5} S / cm at room temperature comparable to that of the well-known conductors $LiAlSiO_4$ and $LiSbO_3$ [39,40]. The structure of the low-temperature modification of $KMgCr(MoO_4)_3$ belongs to the monoclinic system, space group $C2$. The σ value reaches 6×10^{-4} S / cm (932 K). It should be noted that significant cation mobility was revealed not only for compounds with small cation sizes (Li^+, K^+) but also for compounds with much larger cations, such as Cs^+ or Ag^+, situated in cavities of three-dimensional frameworks. For example, $CsCrTi_{0.5}(MoO_4)_3$ compound crystallizing in the $R\bar{3}$ space group possesses an ionic conductivity from 10^{-6} S / cm at 298 K to 10^{-2} S / cm at 780 K. Therefore, not only potassium-containing systems but also thallium-containing systems are of interest.

* Corresponding author.
E-mail address: grossmanv@mail.ru (V.G. Grossman).

https://doi.org/10.1016/j.jallcom.2021.159828
0925-8388/© 2021 Published by Elsevier B.V.

2. Experimental

2.1. Characterization methods

PXRD patterns were recorded on a Bruker D8 ADVANCE X-ray diffractometer (Bruker, Berlin, Germany) with Cu-K_α radiation (λ = 1.5418 Å) at room temperature. The scanning range is between 5° and 100° with a scanning width of 0.02 and a rate of 0.1 s^{-1}.

The variable counting time (VCT) scheme was used to collect the diffraction data. The measurement time was systematically increased towards higher 2θ angles, leading to drastically improved data quality [41,42]. To collect the X-ray data using VCT scheme, five ranges were generated on the diffraction pattern: 5–32.0° (exposure per point: 0.5 s; step: 0.0069°), 32.0–59.0° (exposure per point: 1 s; step: 0.0069°), 59.0–86.0° (exposure per point: 2 s; step: 0.0069°), 86.0–113.0° (exposure per point: 4 s; step: 0.0069°) and 113.0–140° (exposure per point: 8 s; step: 0.0069°). Total experimental time was equal to ~19 h. The esd's σ(I_i) of all points on patterns were calculated using intensities I_i: σ(I_i)=$I_i^{1/2}$. The intensities and obtained esd's were further normalized, taking into account actual value of exposition time, and saved in xye-type file. So transformed powder pattern has usual view in whole 2θ range 5–140º, but all high-angle points have small esd's.

The DSC/TG analysis during heating and cooling was carried out using a calorimeter NETZSCH STA 449 F1 TG/DSC/DTA (Jupiter). The sample charge was 17–18 mg, and the rate of temperature rise was 10 K/min under the Ar atmosphere. All the measurements were made in platinum crucibles. The DSC curves were calculated using a specially developed program from Netzsch.

Electrical conductivity measurements were carried out on cylinder shaped ceramic samples which were 10 mm in diameter and 2 mm thick, with platinum electrodes by the electrochemical impedance method on a *Z*-1500*J* impedance meter in the temperature range about 293–993 K. The test frequency can be set from 1 Hz to 1 MHz at high resolution. Electrical conductivity σ_{total} for each temperature was calculated from:

$$\sigma_{total} = L / R_{total} \times S \quad (1)$$

Where σ_{total}, L, S and R_{total} the total conductivity, the thickness of specimen, and the area of roundsurface and the total resistance, respectively.

Ceramic disks for investigations were prepared by pressing the powders at 100 bar by a PLG-12 hydraulic laboratory press and sintering at 773 K for 2 h. For the making of electrodes, large surfaces of the disks were covered with a paste, which was a mixture of hexachloroplatinate (IV) ammonium $(NH_4)_2[PtCl_6]$ in toluene. Then, the tablet with the applied paste was annealed at a temperature of about 773 K for 1 h.

The geometric to X-ray density ratio was used for evaluation of the density of the ceramics. The geometric density was calculated by dividing the weight of the sintered sample by its volume estimated from geometric dimensions. The size of the sample was measured with an accuracy of ± 0.01 mm. The theoretical density was calculated by the equation,

$$\rho_{x\text{-}ray} = 1.66MZ/V, \quad (2)$$

where M is the molecular weight of the formula unit of a substance, Z is the number of formula units, and V is the unit cell volume.

2.2. Preparation of samples

The following commercial reagents Tl_2CO_3 (chemically pure, Red Chemist, Russia), K_2MoO_4 (chemically pure, Red Chemist, Russia), $Cr(NO_3)_3$ (Joint Stock Company Kyiv Plant of Reagents, Indicators and Analytical Products "RIAP"), HfO_2 (chemically pure, IGIC RAS, Russia), and MoO_3 (chemically pure, Red Chemist, Russia) were used as the starting reagents. The starting reactants were dehydrated at 473 K for a day in a muffle furnace. Simple molybdates Tl_2MoO_4 and $HfMoO_4$ were obtained by annealing the appropriate stoichiometric mixtures of Tl_2CO_3, HfO_2, and MoO_3 at 673–823 K and 673–1023 K, respectively, for 100 h. Because that molybdenum oxide sublimes below the melting point, the synthesis of simple molybdates began at a temperature of 673 K. A stoichiometric mixture of $Cr(NO_3)_3$ and MoO_3 was used for the synthesis of $Cr_2(MoO_4)_3$ at 623–1073 K for 100 h. The annealing was started at a temperature of 623 K to avoid the release of reagents due to the violent evolution of nitrogen oxide and oxygen. The starting reagents were well mixed and ground in an agate mortar with a pestle. To accelerate the interaction, the reaction mixtures were gradually annealed at the temperatures specified in the interval and ground after every 24 h of annealing.

The phase formation in the M_2MoO_4–$Cr_2(MoO_4)_3$–$Hf(MoO_4)_2$ (M = K, Tl) systems was investigated by the cross-section method in the subsolidus region using the literature data on binary systems [47]. Therefore, we did not carry a repeated study of these binary systems. According to Khaikina E.G [43], two double molybdates $KCr(MoO_4)_2$, and $K_5Cr(MoO_4)_4$ composition is formed in the K_2MoO_4–$Cr_2(MoO_4)_3$ system.

Triclinic $KCr(MoO_4)_2$ has a layered structure. Layers $\{[R(MoO_4)_2]^-\}$ run perpendicular to the triple-axis. RO_6 octahedra are located in one layer, in the other – KO_{12}. MoO_4 tetrahedra, having common vertices with RO_6 octahedra, are located in a layer of alkali metal. $K_5Cr(MoO_4)_4$ has a distorted palmierite structure. The system K_2MoO_4–$Cr_2(MoO_4)_3$ is characterized by a non-quasi-binary interaction. This is indicated by the presence of potassium polymolybdate and double potassium and chromium polymolybdate in the annealed reaction mixtures of this system. $TlCr(MoO_4)_2$ phase crystallize in orthorhombic crystal system (space group *Pnma*, Z = 4) [43,44]. The paper Tushinova Yu.L. [45] reports that new compounds are not formed in the system $Cr_2(MoO_4)_3$–$Hf(MoO_4)_2$. The two compounds forming in the K_2MoO_4–$Hf(MoO_4)_2$ system are the congruently melting double molybdates $K_2Hf(MoO_4)_3$ and $K_8Hf(MoO_4)_6$ [46]. $K_2Hf(MoO_4)_3$ and $K_8Hf(MoO_4)_6$ crystallize in the monoclinic structure in space groups $P2_1/m$ and $P2_1/c$, respectively. According to data [47], there are two double molybdates in the system Tl_2MoO_4–$Hf(MoO_4)_2$: $Tl_8Hf(MoO_4)_6$ (monoclinic system, space group $C2/m$) and $Tl_2Hf(MoO_4)_3$.

The verification of the entire subsolidus area in the M_2MoO_4–$Cr_2(MoO_4)_3$–$Hf(MoO_4)_2$ (M = K, Tl) systems consisted of preparing appropriate mixtures of the phases. These mixtures were subjected to long-term heating at temperatures lower than the temperatures of corresponding solidus planes, and next they were cooled to room temperature. The X-ray powder diffraction showed that upon prolonged heating at temperatures close to the melting temperatures, the phase composition of none of these preparations changed. This confirms that the initial mixtures corresponded, as to their composition, to the earlier identified phases coexisting at equilibrium within particular fields of the subsolidus area. This allowed us to determine the quasi-binary joins and detect the formation of new triple molybdates. It should be noted, that the area of the K_2MoO_4–$Cr_2(MoO_4)_3$–$Hf(MoO_4)_2$ system near $K_5Cr(MoO_4)_4$ is necessarily considered as non-quasi ternary. This is due to the presence of potassium polymolybdate and double potassium and chromium polymolybdate. In this connection, the subsolidus triangulation diagram can be constructed for the region $KCr(MoO_4)_2$–$Cr_2(MoO_4)_3$–$Hf(MoO_4)_2$–$K_8Hf(MoO_4)_6$. The results of tests carried out on samples of the basic and control series allowed to determine a phase diagram for the subsolidus area of M_2MoO_4–$Cr_2(MoO_4)_3$–$Hf(MoO_4)_2$ (M = K, Tl) systems in the entire range of component concentrations (Figs. 1 and 2). It can be

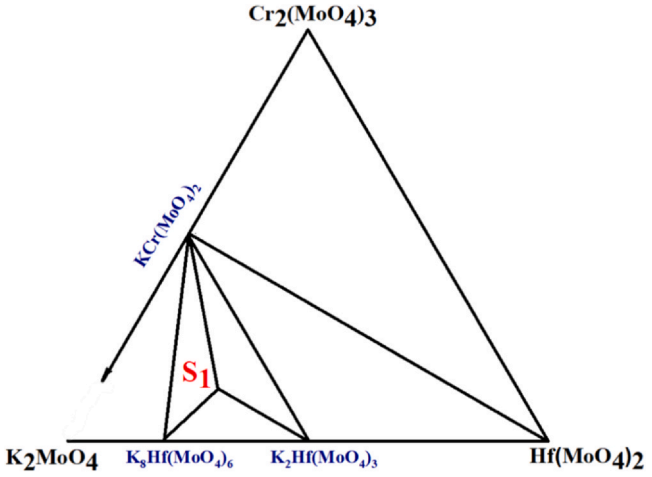

Fig. 1. Phase equilibria of the K_2MoO_4–$Cr_2(MoO_4)_3$–$Hf(MoO_4)_2$ system in the subsolidus region 723–773 K, where S_1 is $K_5CrHf(MoO_4)_6$.

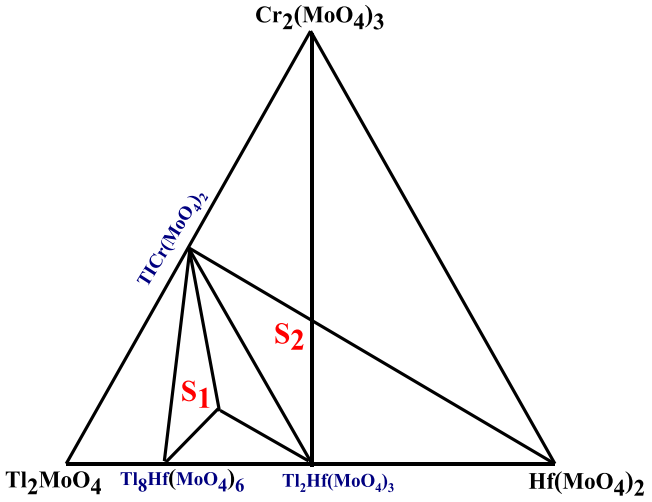

Fig. 2. Phase equilibria of the Tl_2MoO_4–$Cr_2(MoO_4)_3$–$Hf(MoO_4)_2$ system in the subsolidus region 773–823 K, where S_1 is $Tl_5CrHf(MoO_4)_6$ and S_2 is $TlCrHf_{0.5}(MoO_4)_3$.

concluded from the phase diagram presented in Fig. 1 that the subsolidus area of the K_2MoO_4–$Cr_2(MoO_4)_3$–$Hf(MoO_4)_2$ system is composed of five partial subsystems, six quasi binary joins ($KCr(MoO_4)_2$–$K_8Hf(MoO_4)_6$, $KCr(MoO_4)_2$–$K_2Hf(MoO_4)_3$, $KCr(MoO_4)_2$–$K_5CrHf(MoO_4)_6$, $K_5CrHf(MoO_4)_6$–$K_8Hf(MoO_4)_6$, $K_5CrHf(MoO_4)_6$–$K_2Hf(MoO_4)_3$, $KCr(MoO_4)_2$–$Hf(MoO_4)_2$), and one new triple molybdate. Eight subsystems, nine quasi-binary joins ($TlCr(MoO_4)_2$–$Tl_8Hf(MoO_4)_6$, $TlCr(MoO_4)_2$–$Tl_2Hf(MoO_4)_3$, $TlCr(MoO_4)_2$–$Tl_5CrHf(MoO_4)_6$, $Tl_5CrHf(MoO_4)_6$–$Tl_8Hf(MoO_4)_6$, $Tl_5CrHf(MoO_4)_6$–$Tl_2Hf(MoO_4)_3$, $TlCr(MoO_4)_2$–$TlCrHf_{0.5}(MoO_4)_3$, $Cr_2(MoO_4)_3$–$TlCrHf_{0.5}(MoO_4)_3$, $Hf(MoO_4)_2$–$TlCrHf_{0.5}(MoO_4)_3$, $Tl_2Hf(MoO_4)_3$–$TlCrHf_{0.5}(MoO_4)_3$), and two new triple molybdates of compositions $Tl_5CrHf(MoO_4)_6$ and $TlCrHf_{0.5}(MoO_4)_3$ are formed in the Tl_2MoO_4–$Cr_2(MoO_4)_3$–$Hf(MoO_4)_2$ system (Fig. 2). Oxides of the compounds $M_5CrHf(MoO_4)_6$ (M = K, Tl) were synthesized by reacting K_2MoO_4, $Hf(MoO_4)_2$, $Cr_2(MoO_4)_3$ and Tl_2MoO_4, $Hf(MoO_4)_2$, $Cr_2(MoO_4)_3$ in stoichiometric proportions in the temperature range 723–770 K (for $K_5CrHf(MoO_4)_6$) and 723–793 K (for $Tl_5CrHf(MoO_4)_6$) in air, respectively.

Similarly, $TlCrHf_{0.5}(MoO_4)_3$ was prepared from the constituent oxides $TlCr(MoO_4)_2$, $Hf(MoO_4)_2$ around 873 K in air. The formation of single-phase products was investigated by powder X-ray diffraction (on a Bruker D8 ADVANCE X-ray diffractometer (Bruker, Berlin, Germany) with Cu-Kα radiation (λ = 1.5418 Å)).

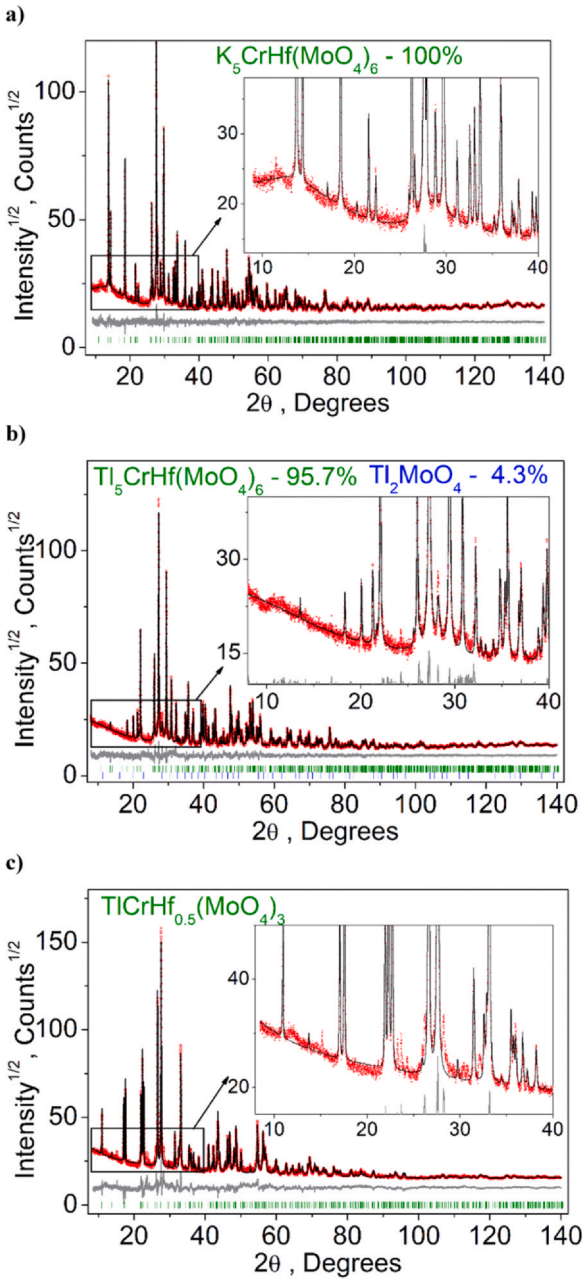

Fig. 3. The X-ray diffraction patterns and the corresponding Rietveld refinement for (a) $K_5CrHf(MoO_4)_6$, (b) $Tl_5CrHf(MoO_4)_6$ and (c) $TlCrHf_{0.5}(MoO_4)_3$ compounds, respectively.

3. Results and discussion

3.1. Crystal structure

XRD spectra together with the Rietveld refinement profiles (analyzed by TOPAS 4.2 [48] software) of the $M_5CrHf(MoO_4)_6$ (M = K, Tl), $TlCrHf_{0.5}(MoO_4)_3$ compounds are illustrated in Fig. 3(a)–(c), respectively. All peaks for $M_5CrHf(MoO_4)_6$ (M = K, Tl) compounds were indexed by trigonal cell ($R\bar{3}c$) with parameters close to $K_5InHf(MoO_4)_6$ [49]. The In^{3+} ion was replaced by Cr^{3+} ion and K^+ ion by Tl^+ ion. The ratio of Hf/Cr in two sites was refined taking into account that the sum of occupancies is equal to 1 in each site. In order to reduce the number of refined parameters, only one thermal parameter was refined for all O atoms.

Table 1
Main parameters of processing and refinement of the $M_5CrHf(MoO_4)_6$ (M = K, Tl) and $TlCrHf_{0.5}(MoO_4)_3$ samples.

Compound	$K_5CrHf(MoO_4)_6$	$Tl_5CrHf(MoO_4)_6$	$TlCrHf_{0.5}(MoO_4)_3$
Sp.Gr.	$R\bar{3}c$	$R\bar{3}c$	$R\bar{3}c$
a, Å	10.45548 (5)	10.53406 (12)	12.9710 (2)
c, Å	37.24614 (3)	37.6837 (5)	11.7825 (2)
V, Å^3	3526.14 (4)	3621.39 (9)	1716.78 (6)
Z	6	6	6
2θ-interval, º	9–140	5–140	9–140
R_{wp}, %	3.18	4.35	6.60
R_p, %	3.65	4.86	7.05
R_{exp}, %	2.37	2.77	2.24
χ^2	1.34	1.57	2.95
R_B, %	2.80	3.32	6.34

The $TlCrHf_{0.5}(MoO_4)_3$ crystallizes in a trigonal structure with the space group of $R\bar{3}$ with parameters close $TlFeHf_{0.5}(MoO_4)_3$ [28].

Refinement was stable and gave low R-factors (Table 1). Coordinates of atoms and main bond lengths are in Table 2 and Table 3 respectively.

The schematic spatial views of the $M_5CrHf(MoO_4)_6$ (M = K, Tl), $TlCrHf_{0.5}(MoO_4)_3$ compounds are presented in Fig. 4. In these structures, Hf^{4+} and Cr^{3+} ions are coordinated to six O^{2-} ions to form a $(Hf,Cr)O_6$ octahedrons, Mo^{6+} ions are surrounded by four neighboring O^{2-} ions in a tetrahedral polyhedron. Each octahedron has common vertices with tetrahedra. The atoms arranged in this way form zigzag channels extended along with the a and b axes, in which thallium and potassium atoms are located, respectively.

The crystallographic data are deposited in Cambridge Crystallographic Data Centre (CSD#2057967–2057969). The data can be downloaded from the site (www.ccdc.cam.ac.uk/data_request/cif).

Table 3
Main bond lengths (Å) of $M_5CrHf(MoO_4)_6$ (M = K, Tl) and $TlCrHf_{0.5}(MoO_4)_3$.

a) Main bond lengths (Å) of $K_5CrHf(MoO_4)_6$			
Mo—O1	1.848 (3)	K1—O3^{ii}	2.716 (6)
Mo—O2	1.868 (4)	K1—O4^{i}	2.902 (5)
Mo—O3	1.753 (6)	K2—O2^{i}	2.934 (4)
Mo—O4	1.586 (5)	K2—O3^{iii}	3.038 (5)
(Hf1/Cr1)—O1	2.033 (5)	K2—O4^{iv}	2.897 (5)
(Hf2/Cr2)—O2^{i}	1.953 (4)		
Symmetry codes: i) -x + 2/3, -y + 1/3, -z + 1/3; (ii) x-1/3, y + 1/3, z + 1/3; (iii) y + 2/3, -x + y + 1/3, -z + 1/3; (iv) -x + y + 2/3, -x + 1/3, z + 1/3			
b) Main bond lengths (Å) of $Tl_5CrHf(MoO_4)_6$			
Mo—O1	1.742 (7)	Tl1—O3^{ii}	2.776 (10)
Mo—O2	1.703 (10)	Tl1—O4^{i}	2.948 (9)
Mo—O3	1.491 (9)	Tl2—O2^{i}	2.994 (7)
Mo—O4	1.513 (7)	Tl2—O4^{iii}	3.134 (8)
(Hf1/Cr1)—O1	2.157 (11)		
(Hf2/Cr2)—O2^{i}	2.131 (10)		
Symmetry codes: (i) -x + 2/3, -y + 1/3, -z + 1/3; (ii) x-1/3, y + 1/3, z + 1/3; (iii) -x + y + 2/3, -x + 1/3, z + 1/3			
c) Main bond lengths (Å) of $TlCrHf_{0.5}(MoO_4)_3$			
Mo1—O1	1.687 (13)	Tl1—O3	2.979 (14)
Mo1—O2	1.739 (17)	Tl1—O4^{i}	3.135 (13)
Mo1—O3	1.826 (9)		
Mo1—O4	1.633 (13)		
(Hf1/Cr1)—O1^{ii}	2.042 (13)		
(Hf1/Cr1)—O2	2.029 (17)		
(Hf1/Cr1)—O3^{iii}	2.029 (12)		
Symmetry codes: (i) -x, -y + 1, -z + 1; (ii) -y + 2/3, x-y + 4/3, z + 1/3; (iii) -x + y, -x + 1, z.			

3.2. Thermal and electrical properties

The green compounds of $K_5CrHf(MoO_4)_6$, $Tl_5CrHf(MoO_4)_6$, and $TlCrHf_{0.5}(MoO_4)_3$ molybdates was subjected to DSC/TG

Table 2
Fractional atomic coordinates and isotropic displacement parameters (Å^2) of $M_5CrHf(MoO_4)_6$ (M = K, Tl) and $TlCrHf_{0.5}(MoO_4)_3$.

a)Fractional atomic coordinates and isotropic displacement parameters (Å^2) of $K_5CrHf(MoO_4)_6$					
Atom	x	y	z	B_{iso}	Occ.
Mo	0.35550 (7)	0.06343 (7)	0.033417 (17)	0.79 (2)	1
Hf1	0	0	0	0.44 (3)	0.795 (3)
Cr1	0	0	0	0.44 (3)	0.205 (3)
Hf2	0	0	0.25	0.43 (5)	0.205 (3)
Cr2	0	0	0.25	0.43 (5)	0.795 (3)
K1	0	0	0.35325 (8)	2.23 (6)	1
K2	0.3817 (3)	0	0.25	2.14 (5)	1
O1	0.1689 (6)	0.0416 (6)	0.03391 (12)	0.79 (10)	1
O2	0.4897 (5)	0.2462 (5)	0.05334 (11)	0.57 (10)	1
O3	0.3549 (6)	0.9095 (7)	0.05229 (13)	2.07 (13)	1
O4	0.3957 (6)	0.0566 (6)	0.99268 (13)	1.65 (13)	1
b) Fractional atomic coordinates and isotropic displacement parameters (Å2) of Tl5CrHf(MoO4)6					
Atom	x	y	z	B_{iso}	Occ.
Mo	0.35664 (17)	0.06422 (17)	0.03390 (3)	1.17 (7)	1
Hf1	0	0	0	0.50 (8)	0.798 (5)
Cr1	0	0	0	0.50 (8)	0.202 (5)
Hf2	0	0	0.25	0.50 (12)	0.202 (5)
Cr2	0	0	0.25	0.50 (12)	0.798 (5)
Tl1	0	0	0.35588 (4)	3.18 (7)	1
Tl2	0.38479 (12)	0	0.25	2.99 (8)	1
O1	0.1791 (12)	0.0364 (12)	0.0343 (3)	1.65 (13)	1
O2	0.4757 (10)	0.2326 (11)	0.0508 (3)	1.65 (13)	1
O3	0.3598 (11)	0.9299 (11)	0.0449 (3)	1.65 (13)	1
O4	0.4078 (11)	0.0520 (11)	0.9972 (2)	1.65 (13)	1
c) Fractional atomic coordinates and isotropic displacement parameters (Å2) of TlCrHf0.5(MoO4)3					
Atom	x	y	z	B_{iso}	Occ.
Tl1	1/3	2/3	0.50475 (14)	1.80 (13)	1
Mo1	0.03640 (14)	0.5131 (4)	0.31349 (16)	1.93 (12)	1
Hf1	1/6	5/6	1/3	1.52 (13)	1/3
Cr1	1/6	5/6	1/3	1.52 (13)	2/3
O1	0.0155 (10)	0.4939 (17)	0.1720 (11)	1.7 (2)	1
O2	0.0838 (12)	0.6558 (15)	0.3644 (13)	1.7 (2)	1
O3	0.1574 (12)	0.4845 (12)	0.3465 (14)	1.7 (2)	1
O4	0.9141 (14)	0.4195 (12)	0.3793 (11)	1.7 (2)	1

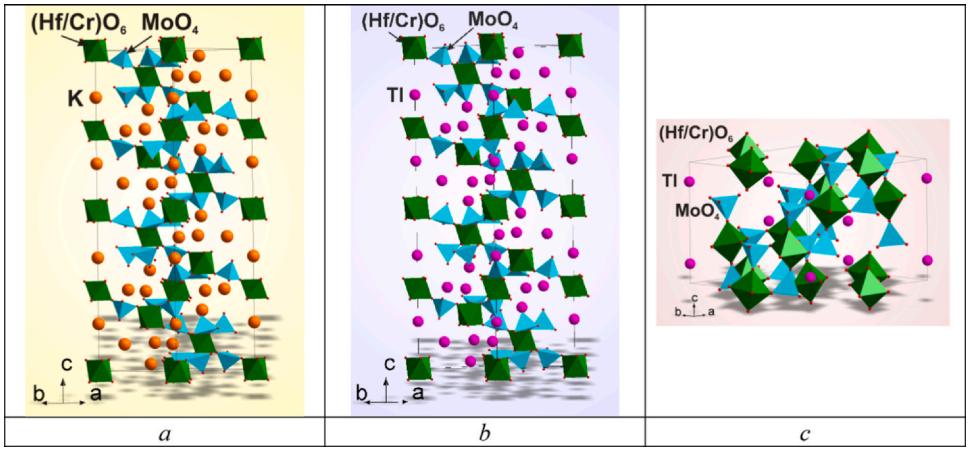

Fig. 4. Crystal structure of (a) $K_5CrHf(MoO_4)_6$, (b) $Tl_5CrHf(MoO_4)_6$ and (c) $TlCrHf_{0.5}(MoO_4)_3$ compounds, respectively.

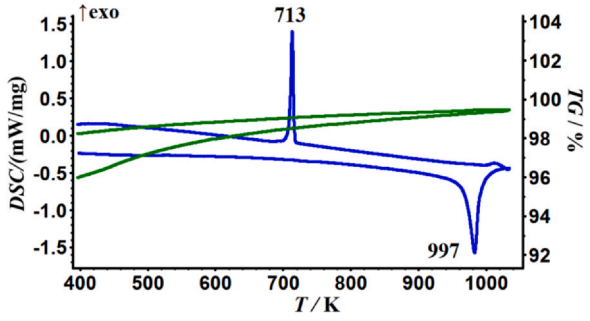

Fig. 5. DSC and TG curves of the $K_5CrHf(MoO_4)_6$.

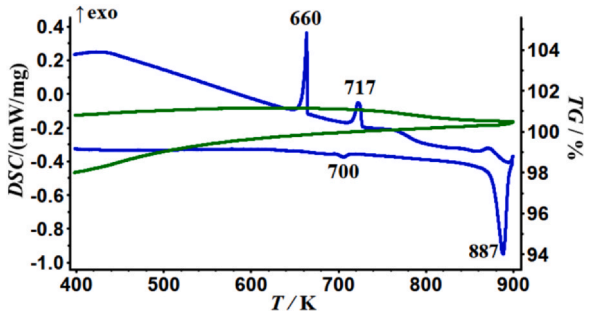

Fig. 6. DSC and TG curves of the $Tl_5CrHf(MoO_4)_6$.

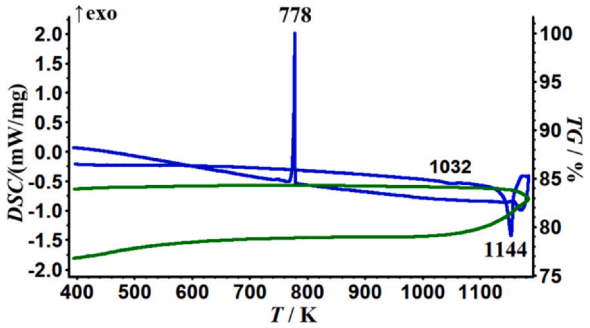

Fig. 7. DSC and TG curves of the $TlCrHf_{0.5}(MoO_4)_3$.

measurements in the argon atmosphere. The results of thermal analysis of the compounds are presented in Figs. 5–7. The TG revealed that no mass loss of $K_5CrHf(MoO_4)_6$, $Tl_5CrHf(MoO_4)_6$, and $TlCrHf_{0.5}(MoO_4)_3$ compounds is observed.

Fig. 5 shows DSC/TG curves of $K_5CrHf(MoO_4)_6$ recorded during heating and cooling runs. The endothermic effect at 997 K is due to the congruent melting of molybdate. The crystallization process from a melt starts at a lower temperature, i.e., 713 K.

The DSC curve of $Tl_5CrHf(MoO_4)_6$ (Fig. 6) revealed two endothermic effects of which the first (a small one) at 700 K, while the second at 887 K. The first effect at 700 K was assigned to the first order phase transition. The second endothermic effect at 887 K relates incongruently melting of the molybdate.

The DSC curve for $TlCrHf_{0.5}(MoO_4)_3$ showed the same as for $Tl_5CrHf(MoO_4)_6$ two endothermic effects, but at significantly higher temperatures (Fig. 7). The first effect is observed at a temperature of 1032 K, and the second, related to the incongruent melting of molybdate, at 1144 K.

Even though that the $K_5CrHf(MoO_4)_6$ and $Tl_5CrHf(MoO_4)_6$ compounds have the same molar composition, the number of effects is different. For comparison, Table 4 shows the thermal characteristics of the molybdates known in the literature with the composition compounds $M_5RHf(MoO_4)_6$ (M = K, Tl; R = Sc, Cr, Fe, In, Bi). It follows from the table that a phase transition appears with an increase in the ionic radius of the monovalent and trivalent elements. The melting points of potassium-containing molybdates are higher than those of thallium-containing ones. In addition, high values of both the melting temperature and the phase transition are observed in molybdates, which include the indium cation.

In this work, additional DSC and TG measurements were also carried out in the air. It was found that the melting point of the potassium compound decreased by 22 K. And for the $Tl_5CrHf(MoO_4)_6$ and $TlCrHf_{0.5}(MoO_4)_3$ compounds the melting point remained the same.Figs. 11 and 12.

The density of the $K_5CrHf(MoO_4)_6$, $Tl_5CrHf(MoO_4)_6$, and $TlCrHf_{0.5}(MoO_4)_3$ ceramics was determined before and after annealing. Sintering of ceramics at high temperatures leads to an increase in density. For example, for $K_5CrHf(MoO_4)_6$, the density of the ceramic increases from 66% (at the outlet of the PLG-12 hydraulic

Table 4
Thermal properties of the compounds $M_5RHf(MoO_4)_6$ (M = K, Tl; R = Sc, Cr, Fe, In, Bi).

Compound	T_{pt}, K	T_m, K	ΔH_{pt}, J/g	ΔH_m, J/g	Ref.
$K_5ScHf(MoO_4)_6$		999		-67.35	[25]
$K_5CrHf(MoO_4)_6$		997		-100.4	this study
$K_5InHf(MoO_4)_6$	910	1015	-1.27	-44.48	[27]
$Tl_5CrHf(MoO_4)_6$	700	878	-0.78	-36.72	this study
$Tl_5FeHf(MoO_4)_6$	690	874	-1.76	-62.42	[29]
$Tl_5InHf(MoO_4)_6$	837	941	-2.27	-7.89	[30]
$Tl_5BiHf(MoO_4)_6$	731	871	-3.15	-41.71	[31]

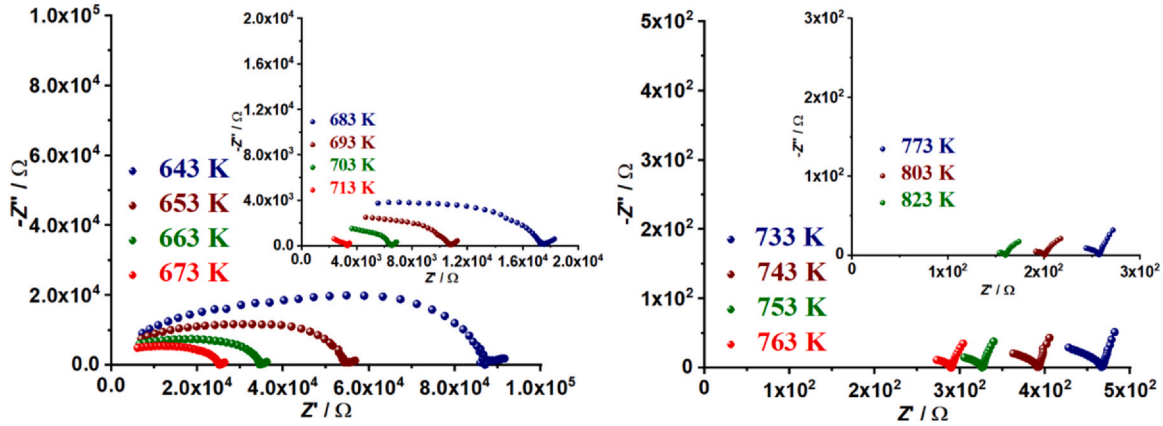

Fig. 8. Impedance spectra of $K_5CrHf(MoO_4)_6$.

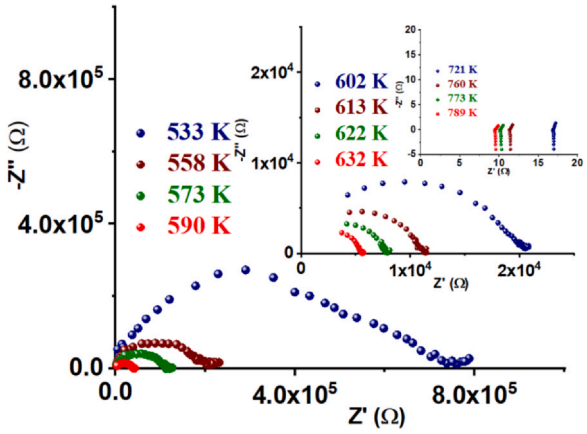

Fig. 9. Impedance spectra of $Tl_5CrHf(MoO_4)_6$.

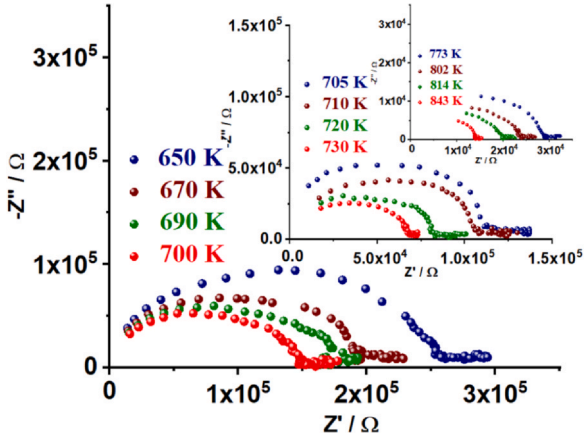

Fig. 10. Impedance spectra of $TlCrHf_{0.5}(MoO_4)_3$.

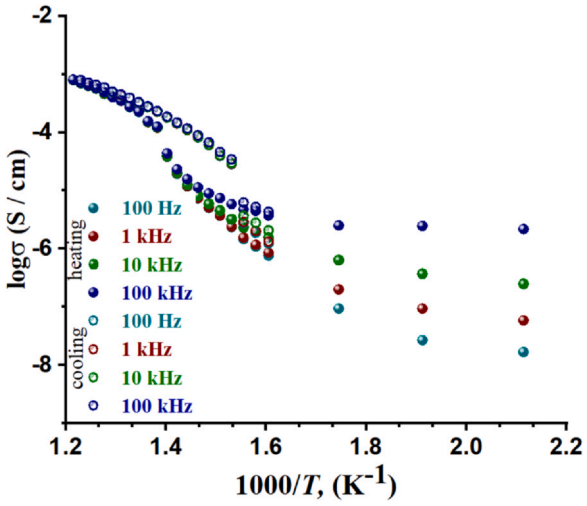

Fig. 11. Dependence of the conductivity of $K_5CrHf(MoO_4)_6$ on frequency and temperature.

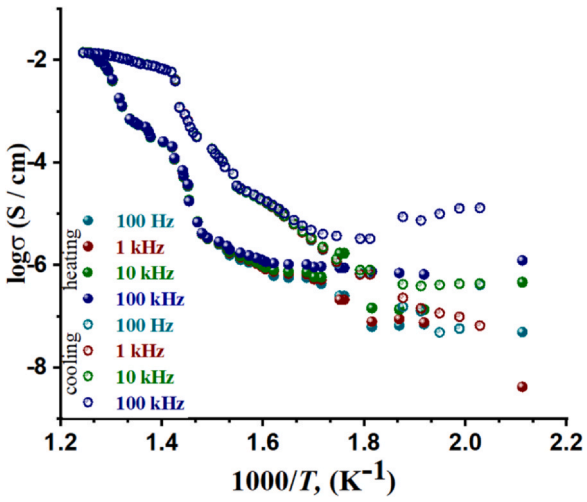

Fig. 12. Dependence of the conductivity of $Tl_5CrHf(MoO_4)_6$ on frequency and temperature.

press) to 79% (after sintering), for $Tl_5CrHf(MoO_4)_6$ from 79% to 86%, and for $TlCrHf_{0.5}(MoO_4)_3$ from 71% to 82%.

The electrical properties of the materials have been investigated by impedance spectroscopy. Complex impedance spectra analysis which represents the Z′ and Z" graphical information for all the molybdates ($K_5CrHf(MoO_4)_6$, $Tl_5CrHf(MoO_4)_6$ and $TlCrHf_{0.5}(MoO_4)_3$) at different temperatures in the air are given in Figs. 8–10, which shows the effect of temperature on impedance behavior. Usually, impedance spectra of a typical electrolyte consist of three semicircles. High frequency and low-frequency semicircles represent grain and material/electrode contribution respectively, and intermediate frequency semicircle represents the grain boundary contribution. In practice sometimes not all the characteristic impedance arcs will be clearly observed in the spectrum. In the impedance plots, the position of the semicircles depends upon the resistance and capacitance values. The capacitance values estimated

Table 5
Potassium and thallium ions conductivity data for $K_5RHf(MoO_4)_6$ (R = Cr, Sc), $Tl_5RHf(MoO_4)_6$ (R = Cr, In, Bi) and $TlCrHf_{0.5}(MoO_4)_3$.

Composition	$\sigma_{573\,K}$ (S/cm)	$\sigma_{773\,K}$ (S/cm)	d_1 (Å)	d_2 (Å)	Ref.
$K_5CrHf(MoO_4)_6$	7.93×10^{-5}	5.22×10^{-4}	3.077(9)	3.128(7)	This study
$K_5ScHf(MoO_4)_6$	2.92×10^{-5}	2.63×10^{-4}	2.996(13)	3.105(10)	[25]
$Tl_5CrHf(MoO_4)_6$	2.94×10^{-4}	1.23×10^{-2}	3.390(17)	3.428(16)	This study
$Tl_5InHf(MoO_4)_6$	3.81×10^{-5}	7.51×10^{-4}	3.185(16)	3.398(14)	[30]
$Tl_5BiHf(MoO_4)_6$	8.35×10^{-7}	4.32×10^{-6}	2.995(13)	3.098(11)	[31]
$TlCrHf_{0.5}(MoO_4)_3$	5.26×10^{-8}	4.42×10^{-6}	3.02(3)	3.09(3)	This study

d_1 is the shortest distance between tetrahedra at room temperature;
d_2 is the shortest distance between tetrahedron and octahedron at room temperature.

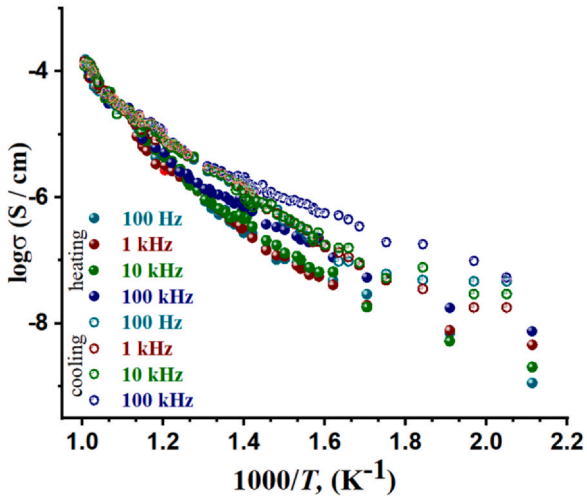

Fig. 13. Dependence of the conductivity of $TlCrHf_{0.5}(MoO_4)_3$ on frequency and temperature.

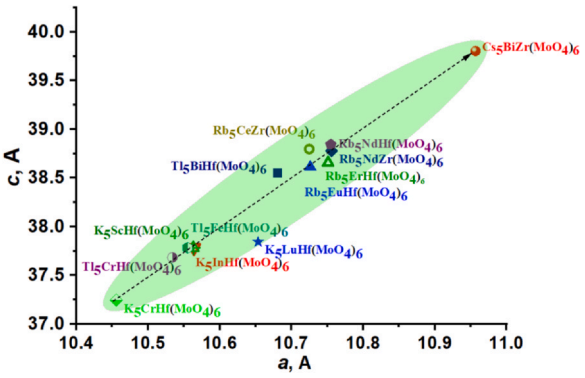

Fig. 14. Dependence of the unit cell parameters.

experimentally from deformed semicircles using the equation $C = 1/2\pi f_{max}R$, where f_{max} is frequency of the peak maxima, have values of 10^{-10} F, which can be considered as the average values of the capacitances for bulk and grain boundary conductivity (10^{-12} and 10^{-8} F). Thus, the semicircle in the -Z'' vs. Z′ plots associated with the sum of both contributions. The diameter of the semicircle decreases with the increase of temperature. A decrease in the grain boundary resistance with increasing temperature suggests the decrease of the barrier to the mobility of charge carriers aiding electrical conduction at higher temperatures. The total conductivity (σ-total) of $K_5CrHf(MoO_4)_6$, $Tl_5CrHf(MoO_4)_6$ and $TlCrHf_{0.5}(MoO_4)_3$ molybdates, was calculated from the inverse of the total resistivity measured in the temperature range from 475 to 830 K for $K_5CrHf(MoO_4)_6$, from 475 to 793 K for $Tl_5CrHf(MoO_4)_6$, and from 475 to 993 K for $TlCrHf_{0.5}(MoO_4)_3$. The curves of the temperature dependence of the conductivity of the $K_5CrHf(MoO_4)_6$ and $Tl_5CrHf(MoO_4)_6$ molybdates have bends in the temperature range 680–780 K for $K_5CrHf(MoO_4)_6$ and 650–800 K for $Tl_5CrHf(MoO_4)_6$, attributed to the phase transition. The dependences of electrical conductivity for many similar solid electrolytes with conduction by monovalent metal cations, studied earlier [21,27,29–31,34,35,37] had a similar shape. In the absence of a phase transition in this temperature range for $K_5CrHf(MoO_4)_6$, following DSC data (Fig. 5), this conductivity jump seems to be due to a change in conduction mechanisms. Perhaps this is because in the high temperature region mobile charge carriers occupy positions accessible to them in disordered. At low temperatures, the cations are arranged in an ordered manner, in the transition region, the cations are gradually disordered with increasing temperature, and the rigid framework remains unchanged. The conductivity of the $Tl_5CrHf(MoO_4)_6$ is higher than that of the $K_5CrHf(MoO_4)_6$ and is 1.1×10^{-2} S / cm at a temperature of 773 K. Above 700 K, the high-frequency semicircles for $Tl_5CrHf(MoO_4)_6$ disappear, which indicates a significant ionic conductivity in ceramics (Fig. 9). These values are

Table 6
Unit cell parameters of triple molybdates $M_5RA(MoO_4)_6$ (M = K, Rb, Cs, Tl; R = Cr, Fe, Sc, In, Bi, Ln; A = Zr, Hf).

Compound	$a = b$	c	V	Z	Sp. gr.	Reference
$K_5CrHf(MoO_4)_6$	10.45548 (5)	37.24614 (3)	3526.14 (4)	6	$R\bar{3}c$	This study
$K_5ScHf(MoO_4)_6$	10.56312(8)	37.6251(3)	3635.74(6)	6	$R\bar{3}c$	[25]
$K_5InHf(MoO_4)_6$	10.564(1)	37.632(4)	3637.0(6)	6	$R\bar{3}c$	[49]
$K_5LuHf(MoO_4)_6$	10.6536(1)	37.8434(8)	3719.75(9)	6	$R\bar{3}c$	[50]
$Tl_5CrHf(MoO_4)_6$	10.53406 (12)	37.6837 (5)	3621.39 (9)	6	$R\bar{3}c$	This study
$Tl_5FeHf(MoO_4)_6$	10.5550 (3)	37.7824 (9)	3645.33 (17)	6	$R1$	[29]
$Tl_5BiHf(MoO_4)_6$	10.6801(4)	38.5518(14)	3808.3(2)	6	$R\bar{3}c$	[31]
$Rb_5ErHf(MoO_4)_6$	10.7511(1)	38.6543(7)	3869.31(9)	6	$R\bar{3}c$	[51]
$Rb_5NdHf(MoO_4)_6$	10.7550(2)	38.8427(13)	3891.0(2)	6	$R\bar{3}c$	[52]
$Rb_5NdZr(MoO_4)_6$	10.7561(2)	38.7790(12)	3885.41(16)	6	$R\bar{3}c$	[53]
$Rb_5CeZr(MoO_4)_6$	10.7248(2)	38.796(1)	3864.52(14)	6	$R\bar{3}c$	[54]
$Rb_5EuHf(MoO_4)_6$	10.7264(1)	38.6130(8)	3847.44(9)	6	$R\bar{3}c$	[55]
$Cs_5BiZr(MoO_4)_6$	10.9569(2)	39.804(4)	4138.4(4)	6	$R\bar{3}c$	[56]

Table 7
Unit cell parameters of triple molybdates $MRA_{0.5}(MoO_4)_3$ (M = Cs, Tl; R = Al, Cr, Fe; A = Zr, Hf).

Compound	$a = b$	c	V	Z	Sp. gr.	Reference
$TlCrHf_{0.5}(MoO_4)_3$	12.9710 (2)	11.7825 (2)	1716.78 (6)	6	$R\bar{3}$	This study
$TlFeHf_{0.5}(MoO_4)_3$	13.0324(2)	11.8083(3)	1736.87(6)	6	$R\bar{3}$	[28]
$CsAlZr_{0.5}(MoO_4)_3$	12.9441(2)	12.0457(4)	1747.86(7)	6	$R\bar{3}$	[57]
$CsFeZr_{0.5}(MoO_4)_3$	13.0876(2)	12.1619(3)	1804.06(6)	6	$R\bar{3}$	[58]

very high for thallium ion conducting solid electrolytes. Table 5 shows that the highest conductivity is in the $Tl_5CrHf(MoO_4)_6$ compound, which has the widest conduction channels in its structure. During the synthesis, thallium fills the channels of the structure, expanding them in comparison with the compound $K_5CrHf(MoO_4)_6$. In the $Tl_5BiHf(MoO_4)_6$ compound, bismuth populates the framework of the structure. The expansion of the octahedron leads to a narrowing of the conduction channel. The most unfavorable situation for ion transport is in the case of the $TlCrHf_{0.5}(MoO_4)_3$ compound. Along the c axis (Tl – Tl distance 3.81 Å), the cations pass through the narrowest part of the channel - between the tetrahedra, the distance is 3.02 (3) Å. It should be noted that the conductivity values for $TlCrHf_{0.5}(MoO_4)_3$ (Fig. 13) are comparable to the conductivity values for $CsMZr_{0.5}(MoO_4)_3$ M^{3+} = Al, In, Sc, Cr, V, Fe [34].

4. Conclusions

Our study of the systems M_2MoO_4–$Cr_2(MoO_4)_3$–$Hf(MoO_4)_2$ (M = K, Tl) revealed a new of trigonal triple molybdates $K_5CrHf(MoO_4)_6$, $Tl_5CrHf(MoO_4)_6$, $TlCrHf_{0.5}(MoO_4)_3$ with three-dimensional frameworks. The basic structural unit of three phases is a three-dimensional mixed framework consisting of $(Cr,Hf)O_6$ octahedra and MoO_4 tetrahedra connected by common oxygen vertices. The thallium and potassium cations occupy wide zigzag channels in the framework extended along the a and b axes. The unit-cell parameters and structural characteristics of the phases have been refined by the Rietveld method. The triple molybdates $K_5CrHf(MoO_4)_6$, $Tl_5CrHf(MoO_4)_6$, along with $M_5RA(MoO_4)_6$ (M = K, Rb, Cs, Tl; R = Cr, Fe, Sc, In, Bi, Ln; A = Zr, Hf), enter into the isostructural series of $K_5InHf(MoO_4)_6$ crystallizing in the space group $R\bar{3}c$. The unit cell parameters of these compounds are presented in Table 6. Fig. 14 shows the dependence of parameters $a = b$ on c. Compounds of this composition known in the literature are located in the ellipsoidal area. We observe a regular increase in parameters from compound $K_5CrHf(MoO_4)_6$ to $Cs_5BiZr(MoO_4)_6$, which are located at the vertices of the ellipse. For this structural type, a significant change in the cell volume by 15% is possible, which creates favorable conditions for the search for new compounds using substitution with other cations.

Molybdate $TlCrHf_{0.5}(MoO_4)_3$ and other molybdates $MRA_{0.5}(MoO_4)_3$ (M = Cs, Tl; R = Al, Cr, Fe; A = Zr, Hf), crystallize in the space group R and are isostructural to $CsAlZr_{0.5}(MoO_4)_3$ [57]. The unit cell parameters of these compounds are presented in Table 7. Unfortunately, these compounds and the $CsAlZr_{0.5}(MoO_4)_3$-type triple molybdates are limited in introducing isomorphic cation and anion substitutions, which is a serious obstacle to enhancing their monovalent-ion conductivity. For compounds $MRA_{0.5}(MoO_4)_3$, in contrast to compounds $M_5RA(MoO_4)_6$, it is possible to change the cell volume by only 5%.

The performed studies allowed us to establish the electrical properties of these compounds. The electroconductivity of the best solid electrolyte that was synthesized in this work is equal to 1.1×10^{-2} S / cm at a temperature of 773 K. The electrical conductivity measurements showed higher values for triple molybdate $Tl_5CrHf(MoO_4)_6$ not only in comparison with molybdates of similar composition [25,27,29–31,37], but also with other known double and ternary molybdates ($\sigma = 7.86 \times 10^{-7}$ S/cm for $Li_{0.87}Na_{0.13}Cr(MoO_4)_2$ at 599 K [59]; $\sigma = 4.8 \times 10^{-6}$ S/cm for $K_3NaCo_4(MoO_4)_6$ at 663 K [60]; $\sigma = 5 \times 10^{-5}$ S/cm for $K_3LiMg_4(MoO_4)_6$ at 673 K; $\sigma = 4.58 \times 10^{-5}$ S/cm for $Na_{0.5}Ni_{0.5}Sc_{1.5}(MoO_4)_3$ at 573 K [61]; $\sigma = 1.63 \times 10^{-2}$ S/cm for $Na_9Al(MoO_4)_{(6)}$ at 803 K [62]). All this relates $K_5CrHf(MoO_4)_6$, $Tl_5CrHf(MoO_4)_6$ to structure types that are promising for the design of new ionic conductors.

CRediT authorship contribution statement

Victoria G. Grossman: Investigation, Writing - original draft preparation, Writing - review & editing. **Maksim S. Molokeev:** Refinement of the structure by the Rietveld method and co-wrote the paper. **Jibzema G. Bazarova:** Conceptualization. **Bair G. Bazarov:** Resources.

Declaration of Competing Interest

The authors declare that they have no known competing financial interests or personal relationships that could have appeared to influence the work reported in this paper.

Acknowledgments

The work was supported by Basic Project of BINM SB RAS №0273-2021-0008. Research was conducted using equipment of the CCU BINM SB RAS (Ulan-Ude, Russia). Structural analysis of materials in this study was partly supported by the Research Grant No. 075-15-2019-1886 from the Government of the Russian Federation.

References

[1] R. Nasri, T. Larbi, M. Amlouk, M.F. Zid, Investigation of the physical properties of $K_2Co_2(MoO_4)_3$ for photocatalytic application, J. Mater. Sci. Mater. Electron. 29 (2018) 18372–18379, https://doi.org/10.1007/s10854-018-9951-x
[2] D.D. Lv, D.F. Zhang, X.P. Pu, M.C. Gao, H.Y. Ma, H.Y. Li, T.T. Zhang, Combustion synthesis of $Li_8Bi_2(MoO_4)_{(7)}$ and photocatalytic properties, Mater. Lett. 144 (2015) 150–152, https://doi.org/10.1016/j.matlet.2015.01.062
[3] Y.T. Lu, Y.Z. Li, Y.L. Huang, C.L. Chen, P.Q. Cai, H.J. Seo, A visible-light-driven photocatalyst of NASICON $Li_2Ni_2(MoO_4)_{(3)}$ nanoparticles, J. Am. Chem. Soc. 98 (2015) 2165–2169, https://doi.org/10.1111/jace.13612
[4] R. Nasri, T. Larbi, M. Amlouk, M.F. Zid, Highly efficient $K_{0.4}Na_{3.6}Co(MoO_4)_{(3)}$ new alluaudite type structure for photocatalytic degradation of methylene blue and green diamine B dyes, J. Mater. Sci. - Mater. Electron. 30 (2019) 9642–9651, https://doi.org/10.1007/s10854-019-01298-w
[5] J.X. Liu, R.J. Wei, J.C. Hu, L.Z. Li, J.L. Li, Novel Bi_2O_3/$NaBi(MoO_4)_{(2)}$ heterojunction with enhanced photocatalytic activity under visible light irradiation, J. Alloy. Compd. 580 (2013) 475–480, https://doi.org/10.1016/j.jallcom.2013.06.154
[6] J. Zhang, D.M. Zhang, R.R. Zhang, Temperature-dependent Raman spectroscopic study of ferroelastic $K_2Sr(MoO_4)$, Chin. Phys. B 27 (2018) 117801, https://doi.org/10.1088/1674-1056/27/11/117801
[7] W. Zapart, M.B. Zapart, Optical studies of the ferroelastic phase transitions in KFe$(MoO_4)_{(2)}$, Phase Transit. 89 (2016) 761–767, https://doi.org/10.1080/01411594.2016.1186274
[8] G.D. Tsyrenova, E.T. Pavlova, S.F. Solodovnikov, N.N. Popova, T.Y. Kardash, S.Y. Stefanovich, I.A. Gudkova, Z.A. Solodovnikova, B.I. Lazoryak, New ferroelastic $K_2Sr(MoO_4)_{(2)}$: synthesis, phase transitions, crystal and domain structures, ionic conductivity, J. Solid State Chem. 237 (2016) 64–71 doi:0.1016/j.jssc.2016.01.011.
[9] M.B. Zapart, W. Zapart, M. Maczka, Complex ferroelastic domain patterns of $K_{1-x}Rb_xSc(MoO_4)_{(2)}$, Cryst. Ferroelectr. 497 (2016) 34–41, https://doi.org/10.1080/00150193.2016.1160729
[10] V.A. Isupov, Ferroelectric and ferroelastic phase transitions in molybdates and tungstates of monovalent and bivalent elements, Ferroelectrics 322 (2005) 83–114, https://doi.org/10.1080/00150190500315574

[11] W. Zapart, M.B. Zapart, Phase transitions in ferroelastic $RbIn(MoO_4)_{(2)}$ at 163 and 143 K, Ferroelectrics 451 (2013) 116–120, https://doi.org/10.1080/00150193.2013.839289

[12] L. Sebastian, Y. Piffard, A.K. Shukla, F. Taulelle, J. Gopalakrishnan, Synthesis, structure and lithium-ion conductivity of $Li_{2-2x}Mg_{2+x}(MoO_4)_3$ and $Li_3M(MoO_4)_3$ (*M* = Cr, Fe), J. Mater. Chem. 13 (2003) 1797–1802, https://doi.org/10.1039/B301189E

[13] I. Ennajeh, M.F. Zid, A. Driss, Synthesis, crystal structure and electrical properties of the molybdenum oxide, J. Crystallogr. 2013 (1–6) (2013) 1–6, https://doi.org/10.1155/2013/146567

[14] R. Nasri, R. Marzouki, S. Georges, S. Obbade, M.F. Zid, Synthesis, sintering, electrical properties and sodium migration pathways of new lyonsite $Na_2Co_2(MoO_4)_3$, Turk. J. Chem. 42 (2018) 1–31, https://doi.org/10.3906/kim-1801-89

[15] P. Loiko, E.V. Vilejshikova, A.A. Volokitina, V.A. Trifonov, J.M. Serres, X. Mateos, N.V. Kuleshov, K.V. Yumashev, A.V. Baranov, A.A. Pavlyuk, Growth, structure, Raman spectra and luminescence of orthorombic $Li_2Mg_2(MoO_4)_3$ crystals doped with Eu^{3+} and Ce^{3+} ions, J. Lumin. 188 (2017) 154–161, https://doi.org/10.1016/j.jlumin.2017.04.021

[16] L. Sebastian, Y. Piffard, A.K. Shukla, F. Taulelle, J. Gopalakrishnan, Synthesis, structure and lithium-ion conductivity of $Li_{2-2x}Mg_{2+x}(MoO_4)_3$ and $Li_3M(MoO_4)_3$ (M^{III} = Cr, Fe), J. Mater. Chem. 13 (2003) 1797–1802, https://doi.org/10.1039/b301189e

[17] E. Ines, G. Samuel, B.S. Youssef, G. Abderrahmen, M.F. Zid, H. Boughazalaa, Synthesis, crystal structure, sintering and electrical properties of a new alluaudite-like triple molybdate $K_{0.13}Na_{3.87}MgMo_3O_{12}$, RSC Adv. 5 (2015) 38918–38925, https://doi.org/10.1039/c5ra02276b

[18] A.K. Ivanov-Shits, A.V. Nistyuk, N.G. Chaban, Electrical conductivity of the mixed molybdates $Li_2M_2^{II}(MoO_4)_{(3)}$ (*M*-II = Cu, Ni, Co) and $Li_3M^{III}(MoO_4)_{(3)}$ (*M*-III = Fe, In, Ga), Inorg. Mater. 35 (1999) 756–758.

[19] A.A. Il'ina, I.A. Stenina, E.P. Kharitonova, A.B. Yaroslavtsev, Phase transitions in double molybdates $K_2M_2^{II}(MoO_4)_{(3)}$ with *M* = Mg or Co, Russ. J. Inorg. Chem. 52 (2007) 1643–1647, https://doi.org/10.1134/S0036023607110010

[20] V.N. Yudin, E.S. Zolotova, S.F. Solodovnikov, Z.A. Solodovnikova, I.V. Korolkov, S. Yu Stefanovich, B.M. Kuchumo, Synthesis, structure, and conductivity of alluaudite-related phases in the Na_2MoO_4–Cs_2MoO_4–$CoMoO_4$ system, Eur. J. Inorg. Chem. 2019 (2019) 277–286, https://doi.org/10.1002/ejic.201801307

[21] N.I. Sorokin, Ionic conductivity of $KMgCr(MoO_4)_3$ molybdate, Cryst. Rep. 62 (2017) 416–418, https://doi.org/10.1134/S106377451703021X

[22] N.M. Kozhevnikova, M.V. Mokhosoev, Triple molybdates, Zh. Neorg. Khim. 37 (1992) 2395–2401.

[23] N.M. Kozhevnikova, M.B. Mosokhoev, Troinye Molibdaty (Ternary Molybdates) Gos. Univ 2000 Buryat, Ulan-Ude.

[24] M.V. Mokhosoev, Zh.G. Bazarova, Complex Molybdenum and Tungsten Oxides with Elements Groups I–IV, Nauka, Moscow, 1990.

[25] V.G. Grossman, J.G. Bazarova, M.S. Molokeev, B.G. Bazarov, New triple molybdate $K_5ScHf(MoO_4)_6$: synthesis, properties, structure and phase equilibria in the M_2MoO_4–$Sc_2(MoO_4)_3$–$Hf(MoO_4)_2$ (*M* = Li, K) systems, J. Solid State Chem. 283 (2020) 121143, https://doi.org/10.1016/j.jssc.2019.121143

[26] E.T. Khobrakova, V.A. Morozov, S.S. Khasanov, G.D. Tsyrenova, E.G. Khaikina, O.I. Lebedev, G. van Tendeloo, B.I. Lazoryak, New molybdenum oxides $Ag_4M_2Zr(MoO_4)_6$ (M = Mg, Mn, Co, Zn) with a channel-like structure, Solid State Sci. 7 (2005) 1397–1405, https://doi.org/10.1016/j.solidstatesciences.2005.08.010

[27] V.G. Grossman, B.G. Bazarov, J.G. Bazarova, $K_5InHf(MoO_4)_6$: A solid state conductor, IOP Conference Series: Earth and Environment Science 320, 2019, 012050.

[28] V.G. Grossman, B.G. Bazarov, R.F. Klevtsova, L.A. Glinskaya, Zh.G. Bazarova, Phase equilibria in the Tl_2MoO_4-$Fe_2(MoO_4)_3$-$Hf(MoO_4)_2$ system and the crystal structure of ternary molybdate $Tl(FeHf_{0.5})(MoO_4)_3$, Russ. Chem. Bull. 61 (2012) 1546–1549, https://doi.org/10.1007/s11172-012-0202-7

[29] N.E. Novikova, V.G. Grossman, B.G. Bazarov, I.A. Verin, A.P. Dudka, S.Yu Stefanovich, J.G. Bazarova, New $Tl_{4.86}Fe_{0.82}Hf_{1.18}(MoO_4)_6$ ternary molybdate: crystal structure and properties, Acta Crystallogr. Sect. B 76 (2020) 839–849, https://doi.org/10.1107/S2052520620010768

[30] V.G. Grossman, J.G. Bazarova, M.S. Molokeev, B.G. Bazarov, Thallium ionic conductivity of new thallium indium hafnium molybdate ceramics, Ionics 26 (2020) 6157–6165, https://doi.org/10.1007/s11581-020-03739-7

[31] V.G. Grossman, S.V. Adichtchev, V.V. Atuchin, B.G. Bazarov, J.G. Bazarova, N. Kuratieva, A.S. Oreshonkov, N.V. Pervukhina, N.V. Surovtsev, Exploration of structural and vibrational properties of ternary molybdate $Tl_5BiHf(MoO_4)_6$ with isolated MoO_4 units and Tl^+ conductivity, Inorg. Chem. 59 (2020) 12681–12689, https://doi.org/10.1021/acs.inorgchem.0c01762

[32] B.I. Lazoryak, V.A. Efremov, Phases of $Na_{2x}Zn_2Sc_{2(1-x)}$-$II(MoO_4)_3$, $Na_{2x}Cd_2Sc_{2(1-x)}$-$II(MoO_4)_3$, $Na_{2x}Mg_2Sc_{2(1-x)}$-$II(MoO_4)_3$ changed composition, Zh. Neorg. Khim. 32 (1987) 652–656.

[33] I.Y. Kotova, N.M. Kozhevnikova, Phase relations in the Na_2MoO_4-$MgMoO_4$-$Cr_2(MoO_4)_3$ system, Inorg. Mater. 34 (1998) 1068–1070.

[34] A.E. Sarapulova, B. Bazarov, T. Namsaraeva, S. Dorzhieva, J. Bazarova, V. Grossman, A. Bush, I. Antonyshyn, M. Schmidt, A.M.T. Bell, M. Knapp, H. Ehrenberg, J. Eckert, D. Mikhailova, Possible piezoelectric materials $CsMZr_{0.5}(MoO_4)_3$ (*M* = Al, Sc, V, Cr, Fe, Ga, In) and $CsCrTi_{0.5}(MoO_4)_3$: structure and physical properties, J. Phys. Chem. 118 (2014) 1763–1773, https://doi.org/10.1021/jp4077245

[35] A. Sarapulova, T. Namsaraeva, D. Mikhailova, B. Schwarz, H. Ehrenberg, Z. Bazarova, B. Bazarov, Structure and magnetic properties of new triple molybdates $CsMZr_{0.5}(MoO_4)_3$ (*M* = Al, Ga, In, Sc, Cr, V, Fe), S191-S191, Acta Crystallogr. A Found. Crystallogr. 66 (2010) s191, https://doi.org/10.1107/S010876731009567X

[36] J.G. Bazarova, Yu.L. Tushinova, B.G. Bazarov, B.E. Oyun, J.D. Angarhayev, Phase equilibrium in the systems Cs_2MoO_4–$R_2(MoO_4)_3$–$Hf(MoO_4)_2$ (*R* = Al, Cr, Fe, Bi, La–Lu), Izv. Vuzov-Prikl. khimiya I Biotekhnol. 8 (2018) 19–28, https://doi.org/10.21285/2227-2925-2018-8-2-19-28

[37] J.G. Bazarova, A.V. Logvinova, B.G. Bazarov, Y.L. Tushinova, S.G. Dorzhieva, J. Temuujin, Synthesis of new triple molybdates $K_5RZr(MoO_4)_6$ (*R* = Al, Cr, Fe, In, Sc) in the K_2MoO_4-$R_2(MoO_4)_3$-$Zr(MoO_4)_2$ systems, their structure and electrical properties, J. Alloy. Compd. 741 (2018) 834–839, https://doi.org/10.1016/j.jallcom.2018.01.208

[38] I.Y. Kotova, S.F. Solodovnikov, Z.A. Solodovnikova, D.A. Belov, S.Y. Stefanovich, A.A. Savina, E.G. Khaikina, New series of triple molybdates $AgA_{(3)}R(MoO_4)_{(5)}$ (*A* = Mg, *R* = Cr, Fe; *A* = Mn, *R* = Al, Cr, Fe, Sc, In) with framework structures and mobile silver ion sublattices, J. Solid State Chem. 238 (2016) 121–128, https://doi.org/10.1016/j.jssc.2016.03.003

[39] U.V. Alpen, E. Schonherr, H. Schultz, G.H. Talat, Beta-eucryptite - one-dimensional LI-ionic conductor, Electrochim. Acta 22 (1977) 805–807, https://doi.org/10.1016/0013-4686(77)80038-8

[40] K. Ozawa, Y. Sakka, M. Amani, Preparation and electrical conductivity measurement of $LiSbO_3$ thin films, Mater. Res. Soc. Symp. Proc. 453 (1997) 617–622.

[41] I. Madsen, R.J. Hill, Variable step-counting times for Rietveld analysis or getting the most out of your experiment time, Adv. X-ray Anal. 35 (1992) 39–47.

[42] I.C. Madsen, R.J. Hill, Collection and analysis of powder diffraction data with near-constant counting statistics, J. Appl. Crystallogr. 27 (1994) 385–392.

[43] E.G. Khaikina, Synthesis, Phase Formation and Structures of Binary and Thernary Molybdates of Single- and Trivalent Metals, D.Sc. thesis, Nikolaev Institute of Inorganic Chemistry, Novosibirsk, 2008.

[44] M.Y. Pleskov, V.A. Morozov, B.I. Lazoryak, M.G. Zhizhin, I.B. Burdakova, K.M. Khal'baeva, G.D. Tsyrenova, E.G. Khaikina, Structures of double molybdates $TlR(MoO4)(2)$ (*R* = In, Sc, Fe, Cr, Al), Russ, J. Inorg. Chem. 50 (2005) 604–614.

[45] Yu.L. Tushinova, J.G., Bazarova, S.I. Arkhincheeva, Phase Equilibria in Systems *R*2(MoO4)3–Zr(MoO4)2, Vsesos. Scientific Reading from Int. Participation, Dedicated. 70th Birthday of Member USSR Academy of Sciences M.V. Mokhosoeva 2002 Publishing House of the BSC SB RAS, 90 91.

[46] E.S. Zolotova, Abstract of the dissertation. Candidate of chemical sciences, Novosibirsk (1986) 25 ([in Russian]).

[47] B.G. Bazarov, R.F. Klevtsova, T.S.T. Bazarova, L.A. Glinskaya, K.N. Fedorov, Zh.G. Bazarova, O.D. Chimitova, Systems Tl_2MoO_4–$E(MoO_4)_2$, where *E* = Zr or Hf, and the crystal structure of $Tl_8Hf(MoO_4)_6$, Russ. J. Inorg. Chem. 51 (2006) 794–799, https://doi.org/10.1134/S0036023606050184

[48] Bruker, AXS TOPAS V4: General Profile and Structure Analysis Software for Powder Diffraction Data. – User's Manual, Bruker AXS, Karlsruhe. Germany, 2008.

[49] B.G. Bazarov, R.F. Klevtsova, T.T. Bazarova, L.A. Glinskaya, K.N. Fedorov, Z.G. Bazarova, Synthesis and crystal structure of triple molybdate $K_5InHf(MoO_4)_6$, Russ. J. Inorg. Chem. 50 (2005) 1146–1149.

[50] E.Yu Romanova, B.G. Bazarov, R.F. Klevtsova, L.A. Glinskaya, Yu.L. Tushinova, K.N. Fedorov, Zh.G. Bazarova, Phase formation in the K_2MoO_4-$Lu_2(MoO_4)_3$-$Hf(MoO_4)_2$ system and the structural study of triple molybdate $K_5LuHf(MoO_4)_6$, Russ. J. Inorg. Chem. 52 (2007) 749–752, https://doi.org/10.1134/S0036023607050154

[51] B.G. Bazarov, R.F. Klevtsova, O.D. Chimitova, L.A. Glinskaya, K.N. Fedorov, Yu.L. Tushinova, Zh.G. Bazarova, Phase formation in the Rb_2MoO_4-$Er_2(MoO_4)_3$-$Hf(MoO_4)_2$ system and the crystal structure of new triple molybdate $Rb_5ErHf(MoO_4)_6$, Russ. J. Inorg. Chem. 51 (2006) 800–804, https://doi.org/10.1134/S0036023606050196

[52] O.D. Chimitova, B.G. Bazarov, R.F. Klevtsova, K.N. Fedorov, L.A. Glinskaya, M.V. Kuznetsov, Z.G. Bazarova, Synthesis, crystal structure, and electrical properties of the new ternary molybdate $Rb_5NdHf(MoO_4)_{(6)}$, Russ. Chem. Bull. 56 (2007) 2135–2139, https://doi.org/10.1007/s11172-007-0337-0

[53] O.D. Chimitova, B.G. Bazarov, K.N. Fedorov, A.V. Dubentsov, L.I. Gongorova, R.F. Klevtsova, L.A. Glinskaya, A.G. Anshits, Crystal structure of triple molybdate in the Rb_2MoO_4-$Nd_2(MoO_4)_3$-$Zr(MoO_4)_2$ system, J. Struct. Chem. 51 (2010) 173–176, https://doi.org/10.1007/s10947-010-0025-z

[54] L.I. Gongorova, B.G. Bazarov, O.D. Chimitova, Z.G. Bazarova, R.F. Klevtsova, L.A. Glinskaya, A.G. Anshits, T.A. Vereschagina, Crystal structure of a new ternary molybdate $Rb_5CeZr(MoO_4)_6$, J. Struct. Chem. 53 (2012) 329–333, https://doi.org/10.1134/S0022476612020175

[55] B.G. Bazarov, O.D. Chimitova, R.F. Klevtsova, Yu.L. Tushinova, L.A. Glinskaya, Zh.G. Bazarova, Crystal structure of a new ternary molybdate in the Rb_2MoO_4-$Eu_2(MoO_4)_3$-$Hf(MoO_4)_2$ system, J. Struct. Chem. 49 (2008) 53–57, https://doi.org/10.1007/s10947-008-0008-5

[56] B.G. Bazarov, T.V. Namsaraeva, R.F. Klevtsova, A.G. Anshits, T.A. Vereshchagina, R.V. Kurbatov, L.A. Glinskaya, K.N. Fedorov, Zh.G. Bazarova, Phase equilibrium in the Cs_2MoO_4- $Bi_2(MoO_4)_3$-$Zr(MoO_4)_2$ system and the crystal structure of new triple molybdate $Cs_5BiZr(MoO_4)_6$, Russ. J. Inorg. Chem. 53 (9) (2008) 1484–1488, https://doi.org/10.1134/S0036023608090222

[57] T.V. Namsaraeva, B.G. Bazarov, R.F. Klevtsova, L.A. Glinskaya, K.N. Fedorov, Zh.G. Bazarova, Subsolidus phase equilibrium in Cs_2MoO_4-$Al_2(MoO_4)_3$-$Zr(MoO_4)_2$ system and crystal structure of new ternary molybdate $Cs(AlZr_{0.5})(MoO_4)_3$, Russ. J. Inorg. Chem. 55 (2010) 209–214, https://doi.org/10.1134/S0036023610020129

[58] B.G. Bazarov, T.V. Namsaraeva, R.F. Klevtsova, V.G. Bamburov, L.A. Glinskaya, Yu.L. Tushinova, Zh.G. Bazarova, K.N. Fedorov, Synthesis and crystal structure of

a new triple molybdate $CsFeZr_{0.5}(MoO_4)_3$, Dokl. Phys. Chem. 431 (2010) 43–47, https://doi.org/10.1134/S0012501610030012

[59] M. Sonni, M.F. Zid, E.K. Hlil, K. Zaidat, C. Rossignol, S. Obbade, Na/Li substitution effect on the structural, electrical and magnetic properties of LiCr(MoO4)2 and β—Li0.87Na0.13Cr(MoO4)2, J. Alloy. Compd. 854 (2021) 154740, https://doi.org/10.1016/j.jallcom.2020.154740

[60] O.A. Gulyaeva, Z.A. Solodovnikova, S.F. Solodovnikov, E.S. Zolotova, Y.G. Mateyshina, N.F. Uvarov, Triple molybdates $K_{3-x}Na_{1+x}M_4(MoO_4)_6$ (M = Ni, Mg, Co) and $K_{3+x}Li_{1-x}Mg_4(MoO_4)_6$ isotypic with II-$Na_3Fe_2(AsO_4)_3$ and yurmarinite: synthesis, potassium disorder, crystal chemistry and ionic conductivity, Acta Crystallogr. Sect. B 76 (2020) 913–925, https://doi.org/10.1107/S2052520620010677

[61] N.M. Kozhevnikova, Synthesis and characterization of a NASICON phase of variable composition $Na_{1-x}Ni_{1-x}Sc_{1+x}(MoO_4)_{(3)}$ ($0 <= x <= 0.5$), Russ. J. Inorg. Chem. 59 (2014) 992–997, https://doi.org/10.1134/S0036023614090113

[62] A.A. Savina, V.A. Morozov, A.L. Buzlukov, I. Yu Arapova, S. Yu Stefanovich, Y.V. Baklanova, T.A. Denisova, N.I. Medvedeva, M. Bardet, J. Hadermann, B.I. Lazoryak, E.G. Khaikina, New solid electrolyte $Na_9Al(MoO_4)_{(6)}$: structure and Na^+ ion conductivity, Chem. Mater. 29 (2017) 8901–8913, https://doi.org/10.1021/acs.chemmater.7b03989